IN-PLANE AND THROUGH-PLANE POROSITIES IN NONWOVENS

Vincent Perna and Dr. A. K. Jena
Porous Materials, Inc.
83 Brown Road
Ithaca, NY 14850

Abstract

Many industrially important nonwovens such as filter materials, felts, paper, battery separators, and hygienic items are produced in the form of sheets. In the past, their porosities have commonly been determined by measuring their characteristics in the direction that points most directly through the sheet. Depending, however, on the process by which the material is manufactured, the porosity measured in the direction piercing the sheet, that is, orthogonal to the plane, may differ from the porosity measured isotropically parallel to the plane of the sheet. We can term these two: Through-plane porosity and In-plane porosity. With certain nonwovens, it appears that there may also be unequal porosities in orthogonal directions within the plane itself. Thus, when seeking to make a proper design of other products using these materials, it can be essential to have the appropriate test data on these different porosities. To accomplish this, test equipment has been devised to measure the Bubble Point in planar nonwovens in both the through-plane and the in-plane directions. The equipment yields reproducible data for both. In a presently used test method for in-plane porosity, the air pressure that is applied is certainly isotropic, however the resulting fluid flow is not. The resulting flow can be greater in some directions than others, depending in part upon the local packing-density of small straight fibers, the loft induced by curled fibers, the primary orientation and length of large fibers, and the uniformity of distribution of all three. The wet-area versus dry-area patterns displayed during in-plane testing provide information on the uniformity of fiber distribution in the manufacturing process.

INTRODUCTION

Many industrially important nonwovens such as paper, filters, battery separators, hygienic items, and others have applications for which information on the anisotropy of their porosity can be important to those who use them *as-is*, or who incorporate them into other products. The performance of the resulting composite can depend upon the relative magnitudes of their material's permeabilities in different directions. Thus, to do a proper design requires getting the appropriate data for the intended application.

Nonwovens are typically produced in the form of sheets, and the porosity in the shortest direction piercing the sheet (through-plane porosity) can be different from that parallel to the surface of the sheet (in-plane porosity). In some nonwovens, there may also be a difference in the in-plane porosity in the direction that the mat is moving as it is being produced versus the in-plane porosity orthogonal to the direction movement of the mat.

The through-plane characteristics of planar materials are specified in part by measuring the Bubble Point pressure. For such a measurement, a sample is soaked in a wetting liquid so as to fill all the pores in the material, and then gas pressure is applied on one side of the sample to force the liquid out of the other side in the thickness direction. The minimum pressure required to initiate flow through the sample is recorded as the Bubble Point pressure. {See Ref. [1].}

To obtain the porosity of the in-plane direction, however, requires a different arrangement in the test chamber---one that can detect flow parallel to the surface of the sheet. The data obtained for these diverse directions can be appreciably different from one another.

For many practical applications, what will be most important is not the Bubble Point pressure of the one largest pore found in each of several different directions, but rather: What is the maximum fluid-transport capability of the total matrix in each of several different directions, individually? For this, the Pore Diameter Distribution data can be a more important parameter, for it reveals the relative quantities of large-, medium-, and small-diameter paths, and this will relate to the speed with which quantities of fluid can be moved. However, the Bubble Point data will tell you: Of the innumerably many tunnels that the air-driven fluid hunted through to find a way out, this is the upper limit on pore size that it found, the very largest diameter path that you will deal with.

EXPERIMENTAL

A computer automated PMI Capillary Flow Porometer [2,3], whose sample chamber was suitably modified, was employed for all tests. It is capable of generating and measuring pressures in small intervals and giving highly reproducible values for Bubble Points [4]. The sample chambers used in this study are shown in Figure 1

Figure 1(a) shows the arrangement for through-plane Bubble Point testing. A circular sample cut from the material is mounted between two O-rings. One of these rings is in the bottom of the chamber and the other is in the bottom of the insert that is placed on top of the sample. The cap for the chamber is screwed on to apply just sufficient pressure to prevent leakage sideways between the upper and lower O-rings. The cap is supported by the threads of the chamber. When compressed gas is introduced under the sample in the chamber, the gas flows upwards through the sample, and escapes to the atmosphere through the top of the chamber.

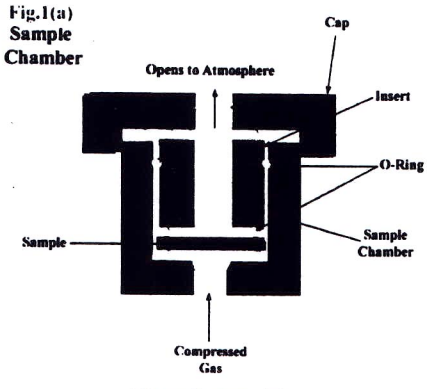

Through-plane (a)

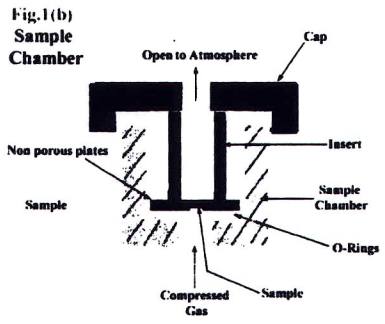

Figure 1(b) shows the arrangement for in-plane Bubble Point testing. The sample is placed between a 5.6 cm diameter non-porous top plate and another 5.6 cm diameter non-porous bottom plate that has a 0.56 cm diameter hole in the center. Compressed gas passes through the central opening in the bottom plate, flows radially within the sample material---parallel to the sandwiching plates---escapes through the holes in the sides of a lightweight insert into the center of the chamber, and exits thence to the atmosphere. Before inserting the sample, it is cut slightly larger in diameter than the plates that will sandwich it and can be immersed continually in a wetting liquid while in the sample chamber. This will allow the sample to automatically rewet itself between subsequent tests at higher compression without the operator having to disturb the material and thereby possibly change its characteristics. The liquid film created between the sample and the non-porous plates has often been adequate to prevent leakage between the plates and the sample. If additional sealing security is desired, sheets of silicone rubber may be installed. Be sure, however, to make the sheet of sample material larger in diameter than the silicone rubber so that when the rubber is under compression it does not bulge out and seal off the edges of the sample, thereby preventing exit of liquid and gas.

For conducting experiments, samples of 6 cm diameter were soaked in the wetting liquid, Porewick™, and placed in the sample chamber. More wetting liquid was added from the top in the sample arrangement shown Figure1(a), and from the sides on the sample edges projecting beyond the non-porous plates in the sample arrangement shown in Figure1(b). After the sample was loaded, the gas pressure was gradually increased until the computer detected flow. The pressure corresponding to the start of flow was recorded by the computer as the Bubble Point pressure.

RESULTS

Bubble Point

Bubble Point parameters measured in the through-plane and in-plane directions were considerably different from one another in the materials tested, as shown in Table 1.

Material Tested	Material Thickness	Bubble Point Pore Diameter (micrometers)		Ratio of Pore Diameters
	millimeters (approx.)	Through-plane	In-plane	
Wrapping Paper (thin)	0.06	26.3	0.96	27.4

Printer Paper	0.08	12.4	1.10	11.3
Photocopier Paper	0.08	9.08	0.73	12.4
"Kraft" envelope paper	0.14	15.5	1.13	13.7
Notepad Backing-Cardboard	0.92	6.70	3.53	1.90
Transmission Fluid Filter Felt (thick, dense)	1.90	80.4	43.3	1.86
Meltblown Sheet (dense)	1.80	114.3	68.8	1.66
Poly Felt Blanket (soft)	2.00	51.8	19.8	2.62
Poly Filter (hard, thin)	0.49	51.1	24.1	2.12
Liquid Filter (thick, hard)	1.50	34.5	15.3	2.25

Table 1.

In doing research and gathering the data in Table 1, it became clear that trying to apply a through-plane value to an in-plane situation could lead to erroneous results. However, as the tests proceeded, a thought-provoking pattern began to emerge. The magnitude of the potential error seemed to be a function of the thickness and porosity of the material being used. Thin, smooth papers had a substantially greater through-plane to in-plane pore diameter ratio (here, averaging about 16). Materials that were six or more times greater in thickness all had ratios around 2.0 in magnitude, which suggests that thinness greatly restricts the path-search options of a pressurized fluid.

Anisotropic in-plane flow: Visual pattern

To find out more about the nature of the fluid flow within a plane, a number of experiments were conducted with a variety of mill-formed, nonwoven sheets, similar to the materials in Table 1. This time, however, instead of recording numbers, the visible progress of drying was observed during a test for in-plane, omnidirectional porosity. Sheet thicknesses ranged from a few thousandths of an inch to over 90 thousandths of an inch. The substances encompassed within the tests were: fairly porous specialty paper for personal correspondence, high-density paper used in laser printers, thin but dense felt used in filtering automotive transmission fluid, battery separator, and, packing-box cardboard that would typically, during use, receive imprinting by ink-jets.

The experiments were set up and started running, but then later were deliberately interrupted before the in-plane Bubble Point pressure had been reached. The cover of the sample chamber was then quickly removed and the sample examined *in-situ* before the fluid could either redistribute itself or evaporate. What was visually quite apparent, especially for thin sheets, was a central portion (nearest the air inlet) that was dry, an outer periphery of the sample disk that was still wet, and a region in between these that exhibited a variety of radially projecting half-dry channels. These three regions are symbolized in Figure 2. Since the liquid that flowed and the air pressure that pushed it

were completely impartial in their efforts to find the easiest path out through the maze of fibers obstructing them, the displayed patterns suggest that in some nonwovens such as paper, cardboard, and thin dense felt, there may be significant non-uniformities in the spatial distribution of thin-&-short versus long-&-thick fibers.

Fig.2

Radial Flow Drying Pattern

MATHEMATICAL ANALYSIS OF THE PHYSICS INVOLVED

In addition to the tests made on substances in our laboratory, we have also made mathematical analyses to try to elucidate the physics behind the visual evidences in the samples tested. This was done in the hope of developing some clarifying scientific theories for such materials and processes. An example of the activity in this regard is described below.

The gas under pressure tries to escape through the sample by displacing the liquid in the openings present in the sample. The paths for gas flow are actually interconnected voids in the sample. The shapes of the voids are very much influenced by the manufacturing process used for the material. For example, battery separators and papers are fibrous, and the structure of one such fibrous battery separator, (Hovosorb) manufactured by Hollingsworth and Vose Company, is shown in the scanning electron micrograph in Figure 3. Such a structure has many unfilled, space-creating openings, which are crisscrossed and penetrated in a random manner by small and large fibers. The surface area in this structure is entirely due to the outer surfaces of fibers. When gas displaces liquid in an opening in such a structure, the extent of the fiber/liquid surface area that is replaced by the fiber/gas surface area is determined by the number of fibers that pass through the space in the opening.

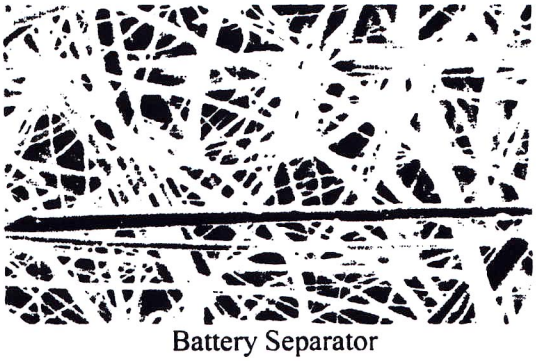

Battery Separator

Fig.4
Gas Containing opening in a fibrous structure

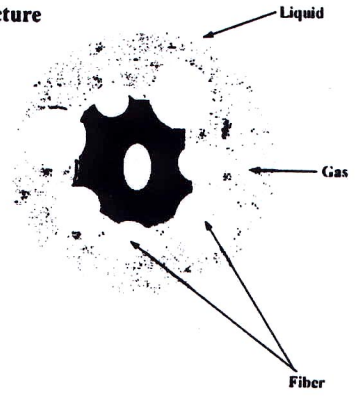

Examining the Thermodynamics

When a wetting liquid is displaced in an opening, the interfacial free energy of the system increases. Therefore, work is done by the gas on the system to provide for the increase in its free energy [5]. Some non-fibrous materials contain openings that enclose empty space within solid walls. In such materials, displacement of the liquid inside the openings leads to an increase of the area of the solid/gas interface at the expense of the solid/liquid interface. The situation is different in a fibrous material. The sketch in Figure 4 illustrates that the displacement of a liquid in an opening in a solid material should lead to increase in two kinds of interfaces: the solid/liquid interface and the liquid/gas interface. Consider a small displacement of the gas inside an opening. Let the increase in the volume of the gas inside the opening be dV, and the increase in the solid/gas and the liquid/gas surface areas be $dS_{s/g}$ and $dS_{l/g}$, respectively. Equating the work done by the gas to the increase in surface free energy:

$$p\,dV = (\gamma_{s/g} - \gamma_{s/l})\,dS_{s/g} + \gamma_{l/g}\,dS_{l/g} \qquad (1)$$

where,

p = pressure of the gas,
$\gamma_{l/g}$ = liquid/gas interfacial free energy,
$\gamma_{s/g}$ = solid/gas interfacial free energy,
$\gamma_{s/l}$ = solid/liquid interfacial free energy.

Eq. (1) may be written as :

$$p = \gamma_{l/g}\,\beta\,(dS_{s/g} / dV)\,[\,1 + (f / \beta)] \qquad (2)$$

where,

$$\beta = (\gamma_{s/g} - \gamma_{s/l}) / \gamma_{l/g}$$

$$f = (dS_{l/g} / dS_{s/g})$$

Fig.5

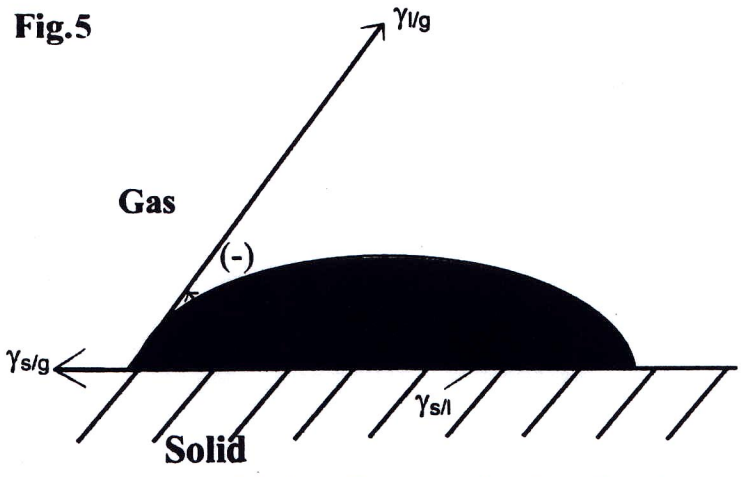

Equilibrium Between Surface Tensions

Equilibrium between the three surface tensions depicted in Figure 5 suggests [6] that:

$$\cos\theta = (\gamma_{s/g} - \gamma_{s/l}) / \gamma_{l/g} \qquad (3)$$

where θ is the contact angle, and $\beta = \cos\theta$. β has a value ≤ 1. However, if the surface free energies are such that equilibrium is not possible, β would be < 1. {See [4].} It has been shown [4] that when wetting liquids with small values of surface free energies are used, β may be taken as 1.

The value of **f** in Equation (2) is not known. However, the magnitude of **f** in a fibrous material may be estimated. Taking approximate values of the maximum opening diameter, fiber diameter, and fiber density from Figure 6, the magnitude of **f** is found to be much less than one. Under these conditions Equation (2) reduces to:

$$p = \gamma_{l/g}\, \beta\, (dS_{s/g} / dV) \qquad (4)$$

For materials, in which openings may be visualized as empty spaces enclosed within solid walls, as in Figure 6, $(dS_{s/g} / dV)$ is equal to (L/A), where **L** is the perimeter of the opening and **A** is the cross-sectional area [4].

Fig.6
Pore enclosed within solid wall

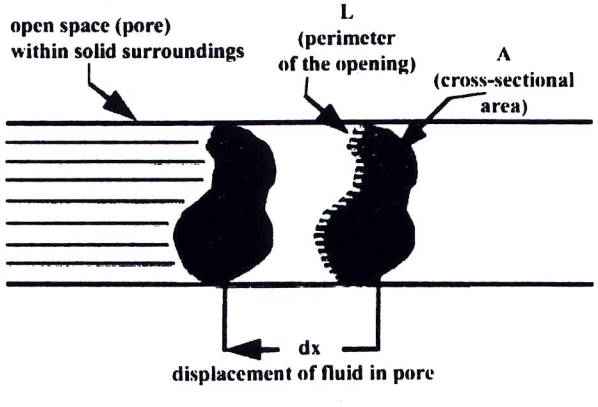

For a specific combination of liquid, gas, and sample material, the interfacial free energies are fixed. Hence, the first two terms on the right hand side of Equation (4) are constants. However, the third term, ($dS_{s/g}$ / dV), is a function of the path of the gas. The gas follows any accessible path. The pressure necessary for the gas to flow along a given path is determined by the highest value of ($dS_{s/g}$ / dV) along that path. The Bubble Point pressure is the pressure required to clear the path through which the gas first escapes the sample. Hence, the Bubble Point pressure is determined by the value of ($dS_{s/g}$ / dV) that is lowest amongst the maxima for all paths.

Equation (4) suggests that the in-plane and the through-plane Bubble Point pressures would not differ appreciably if the fibers were uniformly, randomly oriented. However, the SEM micrograph of Figure 3 suggests that the long dimensions of the largest fibers are mostly parallel to the surface of the sheet. Therefore, the structure of the openings oriented parallel to the surface may be expected to be appreciably different from those traversing the thickness direction, orthogonal to the planar surfaces of the sheet. The measured values in Table 1 seem to confirm this, showing substantial differences between the through-plane and in-plane Bubble Point diameters. The associated Bubble Point pressures, although not listed in the table, reflect this, moving in an inverse relationship to the diameter (D), as shown in Equation [5]:

$$D = 4 \square_{l/g} / p \qquad (5)$$

The first four items in Table 1 are all of the class of paper materials, which are much more densely formed than the battery separator shown in Figure 3. This comes about not only from their materials but also from the calendaring roller-press process, which gives them a much harder, smoother surface. This same process also squashes horizontally oriented pores. Referring to Figure 6, when a horizontal pore is crushed, the cross-sectional area, **A**, is reduced, although the perimeter, **L**, of the pore and the internal surface area of the pore remain constant. With the pore walls now brought closer together, there will be more surface area available per unit volume of liquid than was formerly possible in the pore, and the capillary action of the liquid will be increased in its solid-to-liquid interface (surface tension, $\square_{s/l}$), as in small-diameter pores. Thus it follows from Equation 4 that the amount of gas pressure required to force the liquid out of a crushed pore at the Bubble Point must increase. Correspondingly, the calendared thin-paper materials at the head of Table 1 exhibit radically smaller pores at the Bubble Point than do the bulkier items listed below them in the table. Thus, the experimental setup and the data derived from it behave in exactly the way that the mathematical description of the physics set forth here predicts. This is further exemplified by Figure 2 when the materials tested are thin.

RANDOMNESS OF DISTRIBUTION OF FIBERS

In nonwovens, gas tends to prefer moving along openings in the plane that have the fewest fibers intersecting the opening. Such paths are made possible to some extent by

the longer, larger diameter fibers that provide space near their periphery by their very presence, unless an inordinately large percentage of very small filler-fibers has been introduced to plug up the space near them.

Because of the manner of distribution of the fibers, the periphery of the openings (the surroundings of the paths) in which the gas prefers to move would simulate a solid by having more fibers, and hence, would have less gas. This is seen in Figure 2. If all the fibers, short & long, narrow & fat, were truly randomly distributed, there would be no preferential direction of fluid-flow. The largest, heaviest fibers tend to settle gravitationally such that their long dimensions lie parallel to the plane and are thus these fibers are not uniformly randomly distributed in spatial orientation. With truly random distribution of fibers, in-plane flow from a central point radially outward would produce a smoothly expanding circle of dry area. However, Figure 2, which is a general representation of the irregularities seen in the expanding dry area, clearly demonstrates that the fibers in the mats produced by various mills are not uniformly distributed. The patterns that are seen suggest that areas that are densest and most flow-resistant may have high concentrations of fibers that are clumped together.

If gravity were not an influencing factor in the orientation of fibers within a wet-laid mat, and if the manner of processing in each type of mill had no influence on the directionality of fibers, there would not be statistically skewed distributions of the longest & heaviest and shortest & lightest fibers. Relatedly, if melt-blown processes produced only one specific length and diameter of fiber segments upon a non-moving surface, there would (theoretically) be no preferential directions for fluid flow. Tests in progress, however, suggest that, not only are there differences in the pore-diameters in the in-plane versus through-plane, but there are also differences in the path characteristics in orthogonal directions within a plane. These may be related to the direction and speed of movement of the screen under the fibers that are settling in the slurry for wet-laid mill mats while they are being formed. Also, if meltblown fibers tend to fly through the air with an orientation that retains their alignment with the axis of the ejector nozzle, then the speed of rotation of the drum where they are deposited may have an influence on the orientation in which the fibers land (whether linearly or semi- coiled) and thus on the internal structure of the resulting mat. This may produce differences in the porosities that are measured in a direction aligned with the rotation of the drum versus measurement directions aligned with the axis of the drum.

Depending upon the type of nonwoven material produced, the orientation of long fibers versus short within a sheet, the relative quantities of short-, long-, and semi-coiled fibers, and the local concentration of fibers, will all have an influence upon the packing density in the sheet, and upon the ability of a fluid to move easily through the spaces between fibers. Manufacturers of liquid filters and other nonwovens could find instructive a study of the comparative porosities and Bubble Point ratios of multiple colocated sites on one sheet of planar material. It could give information on how statistically uniform these and the fiber relationships that produce them are. If the quantity distribution and spatial orientation of fibers were uniformly random, that ratio would approach unity.

FUTURE WORK

Since the in-plane and through-plane pore diameters at the Bubble Point can be radically different, and their ratios can depend upon factors such as processing and thickness and also on the (in-plane) differences that are possible between "with-axis" and "cross-axis" porosities in meltblowns and other nonwovens, the question might arise: Should the different types of directional data be compared to one another on an equivalent distance-to-distance basis? This may be appropriate where the material is to be used for the identical purpose in all directions, but how often is this the case? Nevertheless, efforts are being made at PMI to try to extend present test techniques to provide that capability, fbecause very often new insights come from such research.

CONCLUSIONS

(1.) Equipment has been fabricated to measure Bubble Point pressures for the cases where:

gas flows directly through the sheet, and
flows parallel to the surface of sheet materials.

(2.) Bubble Point pressures for both in-plane and through-plane flows have been measured in a number of materials. The resulting test data from these orthogonal directions can be appreciably different---even greater than an order of magnitude for paper-thin, calendared materials, but more like a factor of 2 for thicker, softer nonwovens.

(3.) These results are consistent with the void structures of the materials resulting from their fibrous nature. Mathematical methods were applied to try to elucidate the physics involved.

(4.) Although in-plane gas-pressure is applied isotropically from a central point radially, in a number of materials, the resulting fluid flow is not omnidirectionally equal. In some random directions, the flow is strong, while in immediately neighboring regions the flow may be substantially less, which suggests that there is still room for improvement by manufacturers in their control over fiber distribution in the production processes of these materials. A quick visible check for symptoms of non-uniformity has been provided.

(5.) A means of testing for the randomness and uniformity of distribution of fibers in nonwovens has been presented and a numerical ratio has been set forth as a guide and means of gauging that uniformity.

(6.) Appreciable differences measured between the in-plane and through-plane Bubble Point pressures suggest that there are also substantial differences in the in-plane and through-plane porosities, generally. Therefore, for efficient design of materials that incorporate nonwovens, having data only on the through-plane porosity would not be adequate. It is advisable to provide the designer both the through-plane data *and* the two

orientations of in-plane porosity. A study will be made of the appropriateness of comparing the through-plane and in-plane data on an equivalent-distance-to-distance basis.

REFERENCES

1. ASTM Designation: F316-86.

2. Ron V. Webber: Recent Advances in Automated High Accuracy Bubble Point Measurement, Filtration News, Jan/Feb, p.52, 1994.

3. C. Rebecca Stillwell: Recent Advances in Porometry and Porosimetry: Introducing the Microflow Porometer and the Aquapore Porosimeter, Proceedings of the 7th World Filtration Congress, Budapest, Hungary, May, 1996.

4. Vibhor Gupta and Dr. A. K. Jena: Substitution of Alcohol in Porometers for Bubble Point Determination (submitted for publication).

5. K. Denbigh: The Principles of Chemical Equilibrium, Cambridge University Press,1968.

6. A. W. Adamson: Physical Chemistry of Surfaces, Interscience, New York, 1967.